

Effect of miR-27b-3p and Nrf2 in human retinal pigment epithelial cell induced by high-glucose

Qiao-Ling Lai¹, Ting Xie², Wei-Dong Zheng², Yan Huang¹

¹Department of Ophthalmology and Optometry, Fujian Medical University, Fuzhou 350004, Fujian Province, China

²The First Affiliated Hospital of Fujian Medical University, Fuzhou 350004, Fujian Province, China

Correspondence to: Yan Huang. Department of Ophthalmology and Optometry, Fujian Medical University, 88 Jiaotong RD, Taijiang District, Fuzhou 350004, Fujian Province, China. 13960888823@139.com

Received: 2023-01-20 Accepted: 2023-08-02

Abstract

• **AIM:** To determine whether the microRNA-27b-3p (miR-27b-3p)/NF-E2-related factor 2 (Nrf2) pathway plays a role in human retinal pigment epithelial (hRPE) cell response to high glucose, how miR-27b-3p and Nrf2 expression are regulated, and whether this pathway could be specifically targeted.

• **METHODS:** hRPE cells were cultured in normal glucose or high glucose for 1, 3, or 6d before measuring cellular proliferation rates using cell counting kit-8 and reactive oxygen species (ROS) levels using a dihydroethidium kit. miR-27b-3p, Nrf2, NAD(P)H quinone oxidoreductase 1 (NQO1) and heme oxygenase-1 (HO-1) mRNA and protein levels were analyzed using reverse transcription quantitative polymerase chain reaction (RT-qPCR) and immunocytofluorescence (ICF), respectively. Western blot analyses were performed to determine nuclear and total Nrf2 protein levels. Nrf2, NQO1, and HO-1 expression levels by RT-qPCR, ICF, or Western blot were further tested after miR-27b-3p overexpression or inhibitor lentiviral transfection. Finally, the expression level of those target genes was analyzed after treating hRPE cells with pyridoxamine.

• **RESULTS:** Persistent exposure to high glucose gradually suppressed hRPE Nrf2, NQO1, and HO-1 mRNA and protein levels and increased miR-27b-3p mRNA levels. High glucose also promoted ROS release and inhibited cellular proliferation. Nrf2, NQO1, and HO-1 mRNA levels decreased after miR-27b-3p overexpression and, conversely, both mRNA and protein levels increased after expressing a miR-27b-3p inhibitor. After treating hRPE cells exposed to high glucose with pyridoxamine, ROS levels tended to decrease,

proliferation rate increased, Nrf2, NQO1, and HO-1 mRNA and protein levels were upregulated, and miR-27b-3p mRNA levels were suppressed.

• **CONCLUSION:** Nrf2 is a downstream target of miR-27b-3p. Furthermore, the miR-27b-3p inhibitor pyridoxamine can alleviate high glucose injury by regulating the miR-27b-3p/Nrf2 axis.

• **KEYWORDS:** human retinal pigment epithelial cell; high glucose; pyridoxamine; microRNA-27b-3p; NF-E2-related factor 2; NAD(P)H quinone oxidoreductase 1; heme oxygenase-1

DOI:10.18240/ijo.2023.10.04

Citation: Lai QL, Xie T, Zheng WD, Huang Y. Effect of miR-27b-3p and Nrf2 in human retinal pigment epithelial cell induced by high-glucose. *Int J Ophthalmol* 2023;16(10):1582-1588

INTRODUCTION

Rapid diabetic retinopathy (DR) progression leads to dramatic, irreversible vision loss, including recurrent diabetic macular edema and retinal hemorrhage^[1], and is a leading cause of retinal dysfunction in the macular area^[1-2]. Studies have shown that vision loss in DR is associated with macular foveal photoreceptor-retinal pigment epithelial (RPE) cell complex structure destruction^[3-4]. Moreover, DR leads to glucose, lipid, and protein metabolism disorders *in vivo*^[5]; therefore, DR patients' serum has higher oxidized advanced glycation end-product (AGE) levels compared with non-DR patients^[6]. The RPE layer is mainly responsible for photoreceptor metabolism and also forms the outer barrier of the blood retinal barrier^[7]. Thus, RPE cell play an important role in maintaining photoreceptor-RPE complex and the blood retinal barrier function.

NF-E2-related factor 2 (Nrf2) is a transcription factor that activates antioxidant genes and detoxifying enzymes including NAD(P)H quinone oxidoreductase 1 (NQO1) and heme oxygenase-1 (HO-1)^[8]. This pathway has been implicated in DR occurrence and development^[9] and is also associated with AGE metabolism^[10-12]. Under prolonged hyperglycemia, glucose binds to proteins and lipids to produce hard-to-degrade metabolites, such as AGE, that stimulate cells to release

oxygen free radicals and exacerbate oxidative damage^[6]. Pyridoxamine, one form of vitamin B6, suppresses AGE formation^[13], upregulates Nrf2, exerts antioxidant effects, and protects retinal photoreceptor cells^[14-15]. Incidentally, a recent mouse experiment showed that Nrf2 is a direct target of microRNA-27b-3p (miR-27b-3p)^[16]. Furthermore, studies have shown significant miR-27b-3p upregulation in serum from patients with diabetes, non-proliferative DR, and proliferative DR, and its expression correlates with DR stage severity^[17]. In addition, miR-27b-3p from urinary extracellular vesicles is increased in type 2 diabetic nephropathy^[18]. In this study, we set out to determine how high glucose impacts miR-27b-3p, Nrf2, NQO1, and HO-1 in human RPE (hRPE) cell. We verified the regulatory relationship between Nrf2 and miR-27b-3p and evaluated whether pyridoxamine could alleviate high glucose injury through the miR-27b-3p/Nrf2 pathway.

MATERIALS AND METHODS

Cell Culture The hRPE cell line (ARPE-19) was obtained from the Biowing of Shanghai, China and was cultured in standard Dulbecco's modified Eagle's medium (Gibco, Grand Island, NY, USA) supplemented with 10% fetal bovine serum (Gibco, Grand Island, NY, USA), 100 units/mL penicillin, and 100 µg/mL streptomycin (Gibco, Rockville, MD, USA) in a humidified 5% CO₂ incubator at 37°C.

Cell Counting Kit-8 Analysis Cells were cultured in normal glucose (C), 30 mmol/L glucose (H), or 30 mmol/L glucose with pyridoxamine (2, 4, or 6 µmol/L) for 6d in 96-well plates before incubation with cell counting kit-8 (CCK-8) for 2h. Separately, cells were maintained in normal glucose (C), 30 mmol/L glucose (H) for 1, 3, or 6d (H1, H3, H6), or 30 mmol/L glucose with 4 µmol/L pyridoxamine (HP) for 6d and then incubated with CCK-8 (c0039, Beyotime, Shanghai, China) for 2h. After CCK-8 incubation, absorbance at 450 nm was read using a microplate reader (Thermo Multiska, USA). Cellular proliferation rate was calculated by $(OD_{\text{test group}} - OD_{\text{blank group}}) / (OD_{\text{control group}} - OD_{\text{blank group}})$.

Cell Transfection Lentivirus with a multiplicity of infection of 40 was added to cells in 96 well plates for 1d, followed by addition of 1.0 µg/mL puromycin for 96h. Green fluorescent protein expression was abundant and produced high signal on the fluorescence microscope. Stably infected cell lines were selected for subsequent experiments. Those cells lines were maintained in normal glucose followed by transfection of miR-27b-3p overexpression (OE group) or control lentiviral vectors (NC group, Genechem, Shanghai, China) for 4d or in 30 mmol/L glucose followed by transfection of miR-27b-3p inhibitor (H-in group) or control lentiviral vectors (H-con group, Genechem, Shanghai, China) for 6d. We then performed real-time quantitative polymerase chain reaction (RT-qPCR) to confirm miR-27b-3p mRNA expression levels.

RT-qPCR Analysis Total RNA were extracted using Trizol lysis buffer (Dingguo, Beijing, China) and then converted into cDNA using PrimeScript™ Reagent Kit with gDNA (RR047A, Takara, Japan). RT-qPCR were performed using TB Green™ Premix Ex Taq™ (RR820A, Takara, Japan) with the ABI 7500 system (Applied Biosystems, Foster City, CA, USA). MicroRNA was converted into cDNA, and RT-qPCR was performed using Bluge-Loop™ miRNA RT-qPCR Starter Kit (c110211-2, ruibo, Guangdong, China). Data analysis was conducted with SDS system software (7500 system, Applied Biosystems), and β-actin (Sangon, Shanghai, China) or U6 (ruibo, Guangdong, China) endogenous control levels were used to normalize miR-27b-3p (Ruibo, Guangdong, China), Nrf2, NQO1, and HO-1 (Sangon, Shanghai, China) expression levels. All reactions were performed in triplicate. The results are presented as $2^{-\Delta\Delta Ct}$ means±standard deviation (SD). The following primer sequences were used: miR-27b-3p forward 5'-GCGCGTTCACAGTGGCTAAG-3' and reverse 5'-AGTGCAGGGTCCGAGGTATT-3'; Nrf2 forward 5'-ATCAACTACCCGTTTCGAGAAG-3' and reverse 5'-ACTTGGTCATGTCGATGTCATA-3'; NQO1 forward 5'-AGTATCCTGCCGAGTCTGTTCTGG-3' and reverse 5'-AATATCACAAGGTCTGCGGCTTCC-3'; HO-1 forward 5'-CCTCCCTGTACCACATCTATGT-3' and reverse 5'-GCTCTTCTGGGAAGTAGACAG-3'; β-actin forward 5'-CTCGCCTTTGCCGATCC-3' and reverse 5'-GAATCCTTCTGACCCATGCC; U6 forward 5'-AGAGAAGATTAGCATGGCCCCTG-3' and reverse 5'-ATCCAGTGCAGGGTCCGAGG-3'.

Western Blot Analysis To collect either total protein or nuclear protein, cells were lysed in ice-cold RIPA lysis buffer (WB0061, Dingguo, Beijing, China) or nuclear protein extraction kit buffer (Solarbio, Beijing, China), respectively. Protein obtained from each sample was subjected to sodium dodecyl sulfate polyacrylamide gel electrophoresis (SDS-PAGE) in a Bio-Rad miniature slab gel apparatus (WB0201, Dingguo, Beijing, China) and electrophoretically transferred onto polyvinylidene fluoride membranes (Millipore, Billerica, MA, USA). The polyvinylidene fluoride membranes were then incubated with primary antibodies, including anti-Nrf2 (ab62352), anti-NQO1 (ab80588), anti-HO-1 (ab13243), anti-β-actin (1:1000, ab1001, Abcam, Cambridge, UK), or anti-histone3 (1:1000, H3, 100005-MM01, Yiqiao, Beijing, China), overnight at 4°C, followed by secondary antibody incubation (1:1000, Dingguo, Beijing, China) for 2h at room temperature (RT). Immunoreactive bands were visualized using autoradiography (Bio-Rad, Missisauga, ON, Canada). Protein bands were quantified by densitometry using Image J software. β-actin or H3 protein levels served as internal controls.

Immunocytofluorescence Analysis hRPE cells were cultured in 6-well plates with glass slide for 6d and then fixed with 4% paraformaldehyde for 15min. After permeabilizing with 1% Triton X-100, cells were blocked with 5% bovine serum albumin (A3912, Sigma, USA), incubated with Nrf2, NQO1, or HO-1 antibodies (1:500) overnight at 4°C, and then incubated with secondary antibody (1:1000, ab150083, Alexa Fluor 647, Abcam, Cambridge, UK) for 2h at RT. Images were taken using a positive fluorescence microscope (BX53, Olympus, Tokyo, Japan), and data were analysed using Image J software.

Reactive Oxygen Species Analysis hRPE cells were cultured in 12-well plates for 6d. The medium was then removed, and cells were washed 3 times. The 1 mL per well dihydroethidium (PD-MY 003, MCE, NJ, USA) solution was added, and cells were incubated for 30min in a cell culture incubator, then washed 3 times. Images were taken using an inverted fluorescence microscope (IX71, Olympus, Tokyo, Japan) and 6 fields were randomly selected to represent the reactive oxygen species (ROS) fluorescence intensity. Data were analyzed using Image J software.

Statistical Analysis All results were obtained from at least three independent experiments and presented as mean±SD. Comparisons among groups were tested using one-way ANOVA followed by Bonferroni correction and Tamhane's T2 post-hoc test. All results were analyzed using SPSS 24.0 software (IBM, Amonk, NY, USA) and GraphPad Prism 6.0 software (GraphPad software, La Jolla, CA, USA). $P < 0.05$ was considered statistically significant.

RESULTS

High Glucose Affects miR-27b-3p and Nrf2 Expression As incubation time increased, cellular proliferation rate gradually decreased and ROS content increased in high glucose medium (Figure 1A, 1F, and 1H). After high glucose treatment for 1, 3, or 6d (groups H1, H3, and H6, respectively), the relative miR-27b-3p mRNA expression was higher in the H1 group, but was not significantly different than the control (C) group (Figure 1B). We then assessed Nrf2, NQO1, and HO-1 expression by RT-qPCR, immunocytofluorescence (ICF), and Western blot. We found that Nrf2, NQO1, and HO-1 mRNA levels were upregulated in the H1 group compared to the C group. Conversely, these genes were downregulated in the H6 group compared to the H1 group (Figure 1B). We then calculated protein levels by measuring Western blot band intensity. Compared to the C group, Nrf2 total protein and nuclear protein levels were increased in the H1 group; however, Nrf2 was significantly decreased in the H6 group compared to the H1 group (Figure 1C–1E, 1G). Moreover, ICF revealed positive Nrf2, NQO1, and HO-1 staining in hRPE cells, and we could calculate protein expression levels based on fluorescence

intensity (Figure 1C, 1D). Notably, NQO1 and HO-1 protein levels declined in the H6 group compared to the H1 group; however, H1 group levels were not statistically different than C group levels (Figure 1D).

miR-27b-3p Lentiviral Overexpression or Inhibition Affects Nrf2 Levels After lentiviral miR-27b-3p overexpression (OE group), we found that miR-27b-3p mRNA was significantly increased and Nrf2, NQO1, and HO-1 mRNA levels were reduced compared to the miR-27b-3p control lentiviral (NC group) by RT-qPCR (Figure 2A). In contrast, after miR-27b-3p inhibitor lentiviral transfection (H-in group), we observed strong Nrf2, NQO1, and HO-1 fluorescence in hRPE cells, and Nrf2, NQO1, and HO-1 mRNA and protein were significantly upregulated as measured by RT-qPCR and ICF, respectively (Figure 2B–2D). Additionally, we calculated Nrf2 total protein and nuclear protein expression levels based on Western blot protein band intensity and found that they were upregulated compared to the miR-27b-3p control lentiviral (H-con group, Figure 2E, 2F).

Pyridoxamine Protects hRPE Cells from High Glucose Exposure Effects We applied pyridoxamine to hRPE cultures after high glucose exposure and then analyzed proliferation rates and ROS levels using CCK-8 and dihydroethidium, respectively. We found that hRPE proliferation was greatest after applying 4 μmol/L pyridoxamine compared to 2 or 6 μmol/L pyridoxamine (Figure 3A). Compared to the H group, the proliferation rate was higher and ROS content was significantly lower after 4 μmol/L pyridoxamine application (Figure 3B–3D). Furthermore, we observed strong Nrf2, NQO1, and HO-1 fluorescence and Nrf2 protein band intensity in hRPE cells by ICF and Western blot, respectively (Figure 3F, 3I). We found significant Nrf2, NQO1, and HO-1 mRNA and protein upregulation, including Nrf2 nuclear protein levels in the HP group compared to the H group (Figure 3G, 3H). In contrast, miR-27b-3p mRNA was dramatically downregulated (Figure 3E).

DISCUSSION

Metabolite accumulation and inflammatory factor release are associated with DR progression and likely trigger structural and functional destruction of all retinal layers^[5]. Our work here demonstrated that continuous high glucose exposure gradually increased ROS levels in hRPE cells, which then inhibited normal cellular function and proliferative activity. ROS are a main oxygen radical component and can cause oxidative stress damage^[19-20]. Nrf2 is a strong antioxidant factor *in vivo* that can activate related antioxidant target genes, such as HO-1, NQO1, and glutamate-cysteine ligase catalytic subunit, and scavenge oxygen radicals^[8,21]. Although we found that Nrf2 expression was transiently upregulated after 1d of

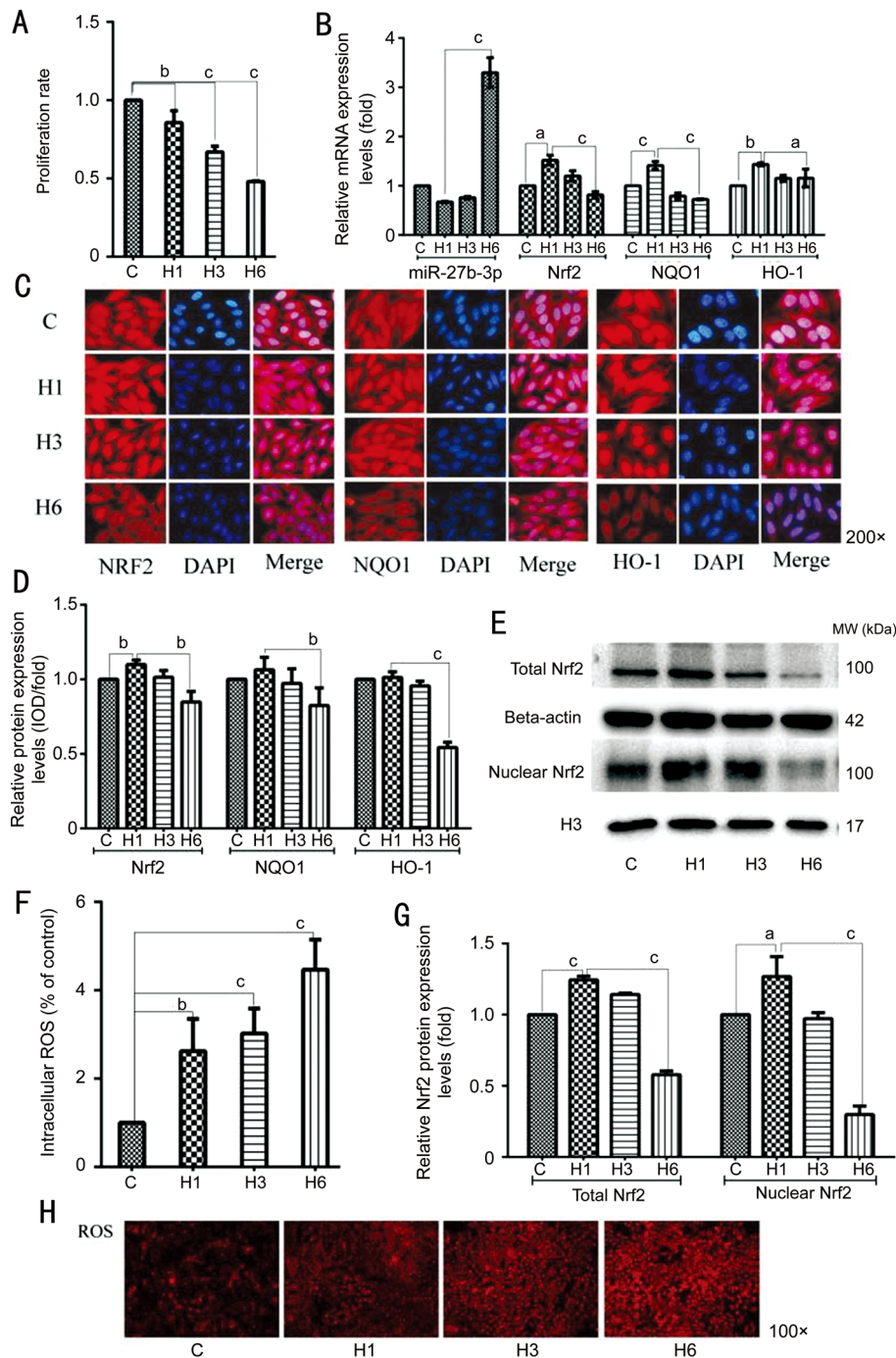


Figure 1 Impact of high glucose exposure for 1, 3, or 6d on hRPE cells A: Cellular proliferation rates; B: Relative miR-27b-3p, Nrf2, NQO1, and HO-1 mRNA levels; C: ICF of Nrf2, NQO1, and HO-1 (200×); D: Semi-quantitative Nrf2, NQO1, and HO-1 ICF protein levels; E: Nrf2 Western blot protein bands from total protein and nuclear protein; F: Intracellular ROS levels; G: Semi-quantitative Nrf2 total protein and nuclear protein Western blot analysis; H: ROS fluorescence (100×). ^a*P*<0.05; ^b*P*<0.01; ^c*P*<0.001. hRPE: Human retinal pigment epithelial; miR-27b-3p: microRNA-27b-3p; Nrf2: NF-E2-related factor 2; NQO1: NAD(P)H quinone oxidoreductase 1; HO-1: Heme oxygenase-1; ICF: Immunocytofluorescence; ROS: Reactive oxygen species; C: Normal glucose group; H1, H3, H6: 30 mmol/L glucose for 1, 3, or 6d groups.

high glucose exposure, its function in activating downstream genes NQO1 and HO-1 was partially repressed. With longer high glucose exposure, we observed weaker Nrf2 expression. Studies have shown that Keap1 binds and inactivates Nrf2 in the cytoplasm; Nrf2 dissociates from Keap1 immediately after internal and external stimulation, translocates to the nucleus, and activates downstream target genes^[8]. Because Nrf2 is

mainly active in the cell nucleus^[22], we evaluated both total and nuclear Nrf2 protein levels. Our results indicated that high glucose attenuates nuclear Nrf2 levels. Accordingly, HO-1 and NQO1 activation were also decreased. Previous studies have demonstrated that HO-1 is one of the main oxygen free radical scavenging enzymes^[23], while NQO1 mainly scavenges exogenous metabolites^[24]. Based on this, we speculate that

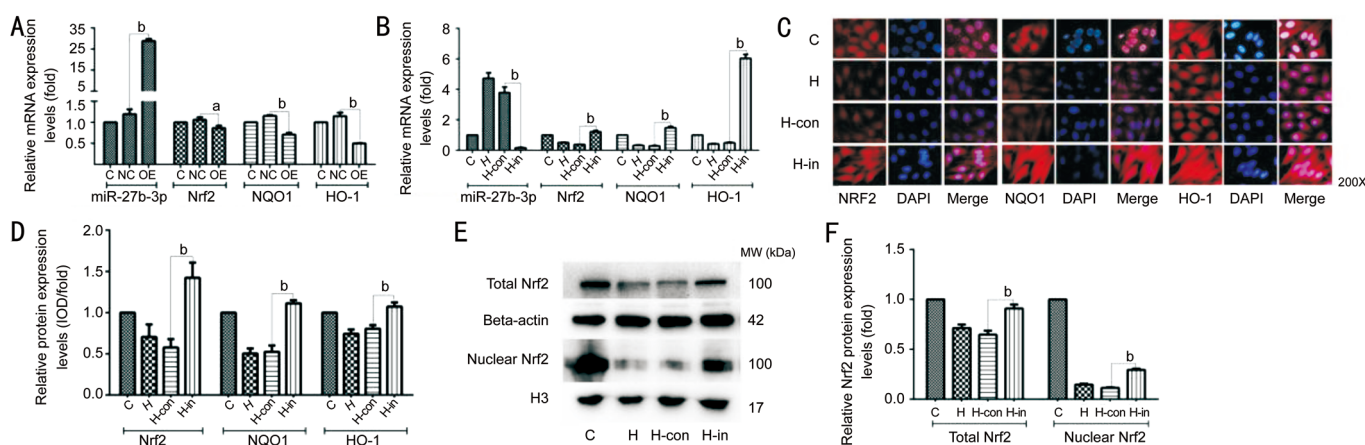


Figure 2 Effects of miR-27b-3p overexpression and inhibition on hRPE cells A: Relative miR-27b-3p, Nrf2, NQO1, and HO-1 mRNA levels after miR-27b-3p overexpression lentiviral transfection; B: Relative miR-27b-3p, Nrf2, NQO1, HO-1 mRNA levels after miR-27b-3p inhibitor lentiviral transfection; C: Nrf2, NQO1, and HO-1 detected by ICF after miR-27b-3p inhibitor lentiviral transfection (200 \times); D: Semi-quantitative Nrf2, NQO1, and HO-1 ICF protein analysis after miR-27b-3p inhibitor lentiviral transfection; E: Nrf2 total protein and nuclear protein bands detected by Western blot after miR-27b-3p inhibitor lentiviral transfection; F: Semi-quantitative Nrf2 total protein and nuclear protein Western blot analysis after miR-27b-3p inhibitor lentiviral transfection. ^a $P < 0.05$; ^b $P < 0.001$. hRPE: Human retinal pigment epithelial; miR-27b-3p: MicroRNA-27b-3p; Nrf2: NF-E2-related factor 2; NQO1: NAD(P)H quinone oxidoreductase 1; HO-1: Heme oxygenase-1; ICF: Immunocytofluorescence; DAPI: 4',6-diamidino-2-phenylindole; C: Normal glucose group; H: 30 mmol/L glucose group; OE: Normal glucose followed by transfection of miR-27b-3p overexpression lentiviral group; NC: Normal glucose followed by transfection of miR-27b-3p control lentiviral group; H-in: 30 mmol/L glucose followed by transfection of miR-27b-3p inhibitor lentiviral group; H-con: 30 mmol/L glucose followed by transfection of miR-27b-3p control lentiviral group.

high glucose promotes ROS deposition by impairing the Nrf2/NQO1/HO-1 axis, resulting in further oxidative stress and ultimately weakening cellular metabolic function.

The microRNAs have been shown to negatively regulate various downstream target genes^[25] and are associated with DR^[26]. Among them, miR-27b is associated with worse DR outcomes^[17-18]. In our experiments, we found that high glucose induced abundant miR-27b-3p expression, which was negatively correlated with Nrf2 expression. Furthermore, Nrf2, NQO1, and HO-1 were dramatically suppressed by miR-27b-3p overexpression. These results suggest that Nrf2 is a downstream target of miR-27b-3p. Therefore, we hypothesized that miR-27b-3p inhibition would activate the Nrf2 axis. Indeed, we found that miR-27b-3p inhibition reversed the phenotypes induced by high glucose. This can mainly be attributed to Nrf2 transfer to the nucleus, followed by heterodimerization with small Maf proteins and binding to antioxidant response elements^[21]. Thus, Nrf2 could enhance antioxidant conduction function, activate NQO2 and HO-1, and possibly reverse the oxidative damage induced by high glucose. Pyridoxamine inhibits AGE^[13] and has been shown to activate Nrf2^[14]. Because 4 $\mu\text{mol/L}$ pyridoxamine conditions resulted in the highest cellular proliferation rate, we chose this concentration for our studies. After pyridoxamine application, hRPE cell were better able to combat high glucose oxidative damage, which was mainly associated with inhibiting miR-

27b-3p and activating the Nrf2 axis. As Nrf2 content increased in the nucleus, its conductive function was enhanced. Consequently, downstream NQO1 and HO-1 could function as antioxidants and reduce ROS accumulation in cells. Oxygen radical scavenging is extremely beneficial for protecting hRPE mitochondrial enzyme activity and for repairing normal cellular metabolic function and maintaining cell proliferation^[27]. We speculate that pyridoxamine's antioxidant mechanisms under high glucose conditions involve inhibiting miR-27b-3p expression, boosting Nrf2 release to the nucleus, and protecting the Nrf2 signaling pathway. Unfortunately, our current work did not examine whether miR-27b-3p and Nrf2 regulation could extenuate AGE deposition, which we plan to investigate in follow-up experiments.

In conclusion, our results suggest that Nrf2 is a downstream target of miR-27b-3p in hRPE cells. Injury from high glucose exposure may be associated with miR-27b-3p upregulation, which promoted Nrf2 degradation or disrupted its nuclear transfer, resulting in reduced NQO1 and HO-1 expression levels. MiR-27b-3p inhibition or pyridoxamine application partially reversed the above phenotypes and alleviated oxidative stress. Accordingly, pyridoxamine may be an miR-27b-3p inhibitor, improving antioxidant effects by regulating miR-27b-3p and Nrf2 and thus protecting hRPE structure and function. Furthermore, miR-27b-3p and Nrf2 could be new therapeutic targets and are worthy of further studies related to novel DR therapy development.

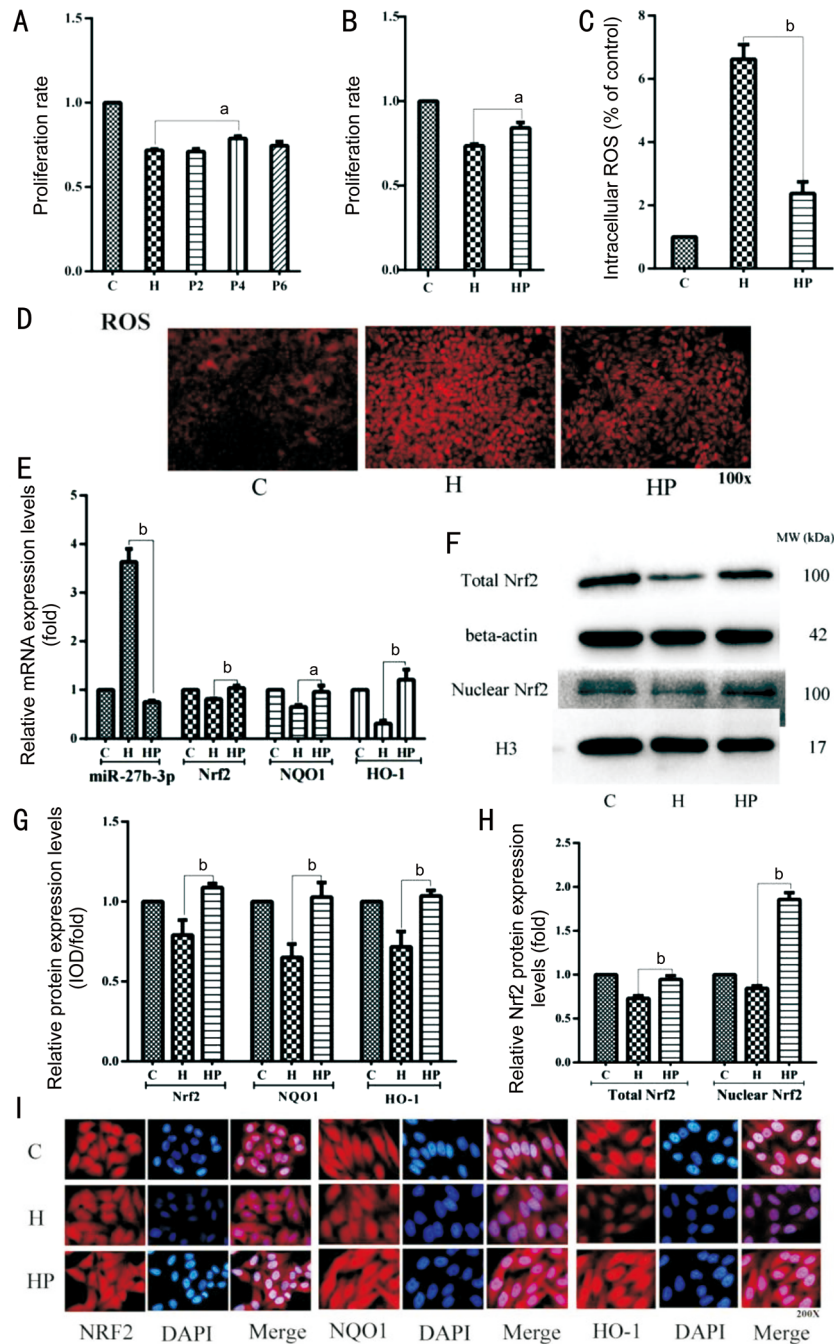


Figure 3 Pyridoxamine protects hRPE cells from high glucose exposure effects A: Cellular proliferation rates after exposure to different pyridoxamine concentrations; B: Cellular proliferation rate after pyridoxamine exposure; C: Intracellular ROS levels; D: ROS fluorescence (100×); E: Relative miR-27b-3p, Nrf2, NQO1, and HO-1 mRNA levels; F: Nrf2 total protein and nuclear protein bands detected by Western blot; G: Semi-quantitative Nrf2, NQO1, and HO-1 protein analysis by ICF; H: Semi-quantitative Nrf2 total protein and nuclear protein analysis by Western blot; I: Nrf2, NQO1, and HO-1 by ICF (200×). ^a*P*<0.01; ^b*P*<0.001. hRPE: Human retinal pigment epithelial; miR-27b-3p: MicroRNA-27b-3p; Nrf2: NF-E2-related factor 2; NQO1: NAD(P)H quinone oxidoreductase 1; HO-1: Heme oxygenase-1; ICF: Immunocytofluorescence; ROS: Reactive oxygen species; DAPI: 4',6-diamidino-2-phenylindole; C: Normal glucose group; H: 30 mmol/L glucose group; P2, P4, P6: 30 mmol/L glucose with pyridoxamine 2, 4 μmol/L, or 6 mol/L; HP: 30 mmol/L glucose with 4 μmol/L pyridoxamine.

ACKNOWLEDGEMENTS

Authors' contributions: Lai QL completed the studies. Lai QL and Xie T wrote the manuscript. Huang Y revised and polished the manuscript. Huang Y and Zheng WD guided the study.

Foundations: Supported by National Natural Science Foundation of China (No.2020J01652); the Training Project

for Young and Middleaged Core Talents in Health System of Fujian Province (No.2016-ZQN-62).

Conflicts of Interest: Lai QL, None; Xie T, None; Zheng WD, None; Huang Y, None.

REFERENCES

1 Sabanayagam C, Banu R, Chee ML, *et al.* Incidence and progression of

- diabetic retinopathy: a systematic review. *Lancet Diabetes Endocrinol* 2019;7(2):140-149.
- 2 Borrelli E, Grosso D, Barresi C, Lari G, Sacconi R, Senni C, Querques L, Bandello F, Querques G. Long-term visual outcomes and morphologic biomarkers of vision loss in eyes with diabetic macular edema treated with anti-VEGF therapy. *Am J Ophthalmol* 2022;235:80-89.
- 3 Tarchick MJ, Cutler AH, Trobenter TD, *et al.* Endogenous insulin signaling in the RPE contributes to the maintenance of rod photoreceptor function in diabetes. *Exp Eye Res* 2019;180:63-74.
- 4 Uji A, Murakami T, Unoki N, Ogino K, Horii T, Yoshitake S, Dodo Y, Yoshimura N. Parallelism for quantitative image analysis of photoreceptor-retinal pigment epithelium complex alterations in diabetic macular edema. *Invest Ophthalmol Vis Sci* 2014;55(5):3361-3367.
- 5 Antonetti DA, Silva PS, Stitt AW. Current understanding of the molecular and cellular pathology of diabetic retinopathy. *Nat Rev Endocrinol* 2021;17(4):195-206.
- 6 Ng Z, Chua K, Iqbal T, Kuppusamy U. Soluble receptor for advanced glycation end-product (sRAGE)/pentosidine ratio: a potential risk factor determinant for type 2 diabetic retinopathy. *Int J Mol Sci* 2013;14(4):7480-7491.
- 7 Cho MJ, Yoon SJ, Kim W, *et al.* Oxidative stress-mediated TXNIP loss causes RPE dysfunction. *Exp Mol Med* 2019;51(10):1-13.
- 8 Yamamoto M, Kensler TW, Motohashi H. The KEAP1-NRF2 system: a thiol-based sensor-effector apparatus for maintaining redox homeostasis. *Physiol Rev* 2018;98(3):1169-1203.
- 9 Radhakrishnan R, Kowluru RA. Long noncoding RNA *MALAT1* and regulation of the antioxidant defense system in diabetic retinopathy. *Diabetes* 2021;70(1):227-239.
- 10 Wang X, Chen X, Zhou W, *et al.* Ferroptosis is essential for diabetic cardiomyopathy and is prevented by sulforaphane via AMPK/NRF2 pathways. *Acta Pharm Sin B* 2022;12(2):708-722.
- 11 Sampath C, Rashid MR, Sang S, Ahmedna M. Green tea epigallocatechin 3-gallate alleviates hyperglycemia and reduces advanced glycation end products via nrf2 pathway in mice with high fat diet-induced obesity. *Biomed Pharmacother* 2017;87:73-81.
- 12 Do M, Hur J, Choi J, Kim Y, Park HY, Ha S. *Spatholobus suberectus* ameliorates diabetes-induced renal damage by suppressing advanced glycation end products in db/db mice. *Int J Mol Sci* 2018;19(9):2774.
- 13 Ramis R, Ortega-Castro J, Caballero C, Casasnovas R, Cerrillo A, Vilanova B, Adrover M, Frau J. How does pyridoxamine inhibit the formation of advanced glycation end products? the role of its primary antioxidant activity. *Antioxidants (Basel)* 2019;8(9):344.
- 14 Ren X, Sun H, Zhang CH, Li C, Wang JL, Shen J, Yu D, Kong L. Protective function of pyridoxamine on retinal photoreceptor cells via activation of the p-Erk1/2/Nrf2/Trx/ASK1 signalling pathway in diabetic mice. *Mol Med Rep* 2016;14(1):420-424.
- 15 Dai XZ, Yan XQ, Zeng J, *et al.* Elevating CXCR7 improves angiogenic function of EPCs via Akt/GSK-3 β /Fyn-mediated Nrf2 activation in diabetic limb ischemia. *Circ Res* 2017;120(5):e7-e23.
- 16 Huang Y, Huang LX, Zhu GF, Pei ZY, Zhang WM. Downregulated microRNA-27b attenuates lipopolysaccharide-induced acute lung injury via activation of NF-E2-related factor 2 and inhibition of nuclear factor κ B signaling pathway. *J Cell Physiol* 2019;234(5):6023-6032.
- 17 Trotta MC, Gesualdo C, Platania CBM, *et al.* Circulating miRNAs in diabetic retinopathy patients: prognostic markers or pharmacological targets? *Biochem Pharmacol* 2021;186:114473.
- 18 Prabu P, Rome S, Sathishkumar C, Gastebois C, Meugnier E, Mohan V, Balasubramanyam M. MicroRNAs from urinary extracellular vesicles are non-invasive early biomarkers of diabetic nephropathy in type 2 diabetes patients with the 'Asian Indian phenotype'. *Diabetes Metab* 2019;45(3):276-285.
- 19 Giacco F, Brownlee M. Oxidative stress and diabetic complications. *Circ Res* 2010;107(9):1058-1070.
- 20 Hodgkinson AD, Millward BA, Demaine AG. Association of the p22phox component of NAD(P)H oxidase with susceptibility to diabetic nephropathy in patients with type 1 diabetes. *Diabetes Care* 2003;26(11):3111-3115.
- 21 Hirotsu Y, Katsuoka F, Funayama R, Nagashima T, Nishida Y, Nakayama K, Engel JD, Yamamoto M. Nrf2-MafG heterodimers contribute globally to antioxidant and metabolic networks. *Nucleic Acids Res* 2012;40(20):10228-10239.
- 22 Ishii T, Warabi E, Mann GE. Mechanisms underlying Nrf2 nuclear translocation by non-lethal levels of hydrogen peroxide: p38 MAPK-dependent neutral sphingomyelinase2 membrane trafficking and ceramide/PKC ζ /CK2 signaling. *Free Radic Biol Med* 2022;191:191-202.
- 23 Campbell NK, Fitzgerald HK, Dunne A. Regulation of inflammation by the antioxidant haem oxygenase 1. *Nat Rev Immunol* 2021;21(7):411-425.
- 24 Oeseburg H, de Boer RA, Buikema H, van der Harst P, van Gilst WH, Silljé HHW. Glucagon-like peptide 1 prevents reactive oxygen species-induced endothelial cell senescence through the activation of protein kinase A. *Arterioscler Thromb Vasc Biol* 2010;30(7):1407-1414.
- 25 Kantharidis P, Wang B, Carew RM, Lan HY. Diabetes complications: the microRNA perspective. *Diabetes* 2011;60(7):1832-1837.
- 26 Satari M, Aghadavod E, Mobini M, Asemi Z. Association between miRNAs expression and signaling pathways of oxidative stress in diabetic retinopathy. *J Cell Physiol* 2019;234(6):8522-8532.
- 27 Kaarniranta K, Uusitalo H, Blasiak J, *et al.* Mechanisms of mitochondrial dysfunction and their impact on age-related macular degeneration. *Prog Retin Eye Res* 2020;79:100858.